1-1-2014

# A validated thermo mechanical FEM model of bead-on-plate welding

Djarot Darmadi
*University of Wollongong*, dbd991@uowmail.edu.au

A Kiet Tieu
*University of Wollongong*, ktieu@uow.edu.au

John Norrish
*University of Wollongong*, johnn@uow.edu.au

# A validated thermo mechanical FEM model of bead-on-plate welding


## Abstract

This paper is presenting accurate FEM model of bead-on-plate welds of 316L stainless steels through thermo-mechanical analysis. The model was composed using ANSYS Parametric Design Language (APDL) program. In thermal analysis, mixed mode of volumetric thermal load was used to represent moving heat source. Growing weld bead was accommodated in both the thermal and mechanical models using birth and death technique. Melting phenomenon was modelled by low stiffness and zero plastic strain of melting elements. Results from thermal analysis and subsequent mechanical analysis have been validated. Good agreements of predicted temperature histories, temperature field and residual stress with experimental results confirmed the accuracy of the proposed FEM model.



## Keywords

thermo, mechanical, fem, model, bead, plate, validated, welding


## Disciplines

Engineering | Science and Technology Studies


## Publication Details

Darmadi, D. B., Kiet-Tieu, A. & Norrish, J. (2014). A validated thermo mechanical FEM model of bead-on-plate welding. International Journal of Materials and Product Technology, 48 (1-4), 146-166.

# A validated thermo mechanical FEM model of bead-on-plate welding

Djarot B. Darmadi*

Department of Mechanical Engineering,
Brawijaya University,
Malang, Jawa Timur 65145, Indonesia
E-mail: b_darmadi_djarot@yahoo.co.id
*Corresponding author

Anh Kiet-Tieu and John Norrish

Department of Mechanical Engineering,
University of Wollongong,
Wollongong, NSW 2500, Australia
E-mail: ktieu@uow.edu.au
E-mail: johnn@uow.edu.au

**Abstract:** This paper is presenting accurate FEM model of bead-on-plate welds of 316L stainless steels through thermo-mechanical analysis. The model was composed using ANSYS Parametric Design Language (APDL) program. In thermal analysis, mixed mode of volumetric thermal load was used to represent moving heat source. Growing weld bead was accommodated in both the thermal and mechanical models using birth and death technique. Melting phenomenon was modelled by low stiffness and zero plastic strain of melting elements. Results from thermal analysis and subsequent mechanical analysis have been validated. Good agreements of predicted temperature histories, temperature field and residual stress with experimental results confirmed the accuracy of the proposed FEM model.

**Keywords:** FEM model; mixed mode thermal load; residual stress; welding; thermo-mechanical analysis.

**Reference** to this paper should be made as follows: Darmadi, D.B., Kiet-Tieu, A. and Norrish, J. (2014) 'A validated thermo mechanical FEM model of bead-on-plate welding', *Int. J. Materials and Product Technology*, Vol. 48, Nos. 1/2/3/4, pp.146–166.

**Biographical notes:** Djarot B. Darmadi is a Senior Researcher at Brawijaya University. He has received research grants including PEKERTI (2004–2005), Fundamental Research (2006–2007) and PEKERTI (2008–2009). He holds Bachelor degree from Brawijaya University with a final research project: FEM analysis on frame of public bus and Master degree from Gadjah Mada University with final research project: Fatigue crack growth behaviour of welded structure. He is finishing his final research project for PhD at University of Wollongong discussing residual stress of pipeline girth weld joints.

Anh Kiet Tieu is a Professor of Mechanical Engineering at The University of Wollongong. His main research focuses are FEM modelling, macro-micro-nano trybology and rolling technology. He is a Leader of Rolling Technology at Engineering Materials Institute and a Coordinator of Research Centre of Engineering Mechanics at University of Wollongong. He is a Visiting Professor at University of Science and Technology of China, Huazhong University of Science and Technology and Northeastern University, China.

John Norrish is a Professor of Materials, Welding and Joining at The University of Wollongong. He is author of *Advanced Welding Processes*, originally published by the Institute of Physics in 1992 and revised and re-published in 2006. He has more than 150 publications and has received numerous awards including the International Institute of Welding E.O. Paton Prize. He is a member of the Governance Board of the Physical Employment Standards Centre of Excellence and Vice Chairman of the International Institute of Welding Commission XII. He is also the Director of the Defence Materials Technology Centre established in 2008.

This paper is a revised and expanded version of a paper entitled 'Numerical prediction of residual stresses in 316L bead on plate welds' presented at the 15th International Conference on Advances in Materials and Processing Technology, AMPT2012, Wollongong, Australia, 23–26 September 2012.

## 1 Introduction

Recent research trend in welding, following on from improvement to welding machine has been devoted to improving the basic understanding of the welding process, consumable and development of equipment and control and automation (Norrish, 2006). To give deep insight and understanding, finite element method (FEM) was used to analyse a welding process, and once the results have been validated the assumptions adopted in FEM analysis are deemed to be correct. Localised high temperature produced by welding torch causes distortions and residual stress in structures with welded joint, and many efforts have been carried out to minimise or study the detrimental effects of both phenomena. Some researcher focused on the distortion (Smith, 2009; Sudhakaran et al., 2010; Goldak and Asadi, 2011) while the other on the residual stress (Anawa and Olabi, 2008; Akbari and Sattari-Far, 2009; Murakawa et al., 2010; Darmadi, 2011a; Darmadi et al., 2012a) or both phenomena (Moraitis and Labeas, 2008; Xu et al., 2009; Gannon et al., 2010; Sudheesh and Siva Prasad, 2011; Gannon et al., 2012). The residual stress leads to premature fatigue damage, stress corrosion and fracture (Lei et al., 2006; Xu et al., 2007). This paper is following one of the welding research trends: improving the basic understanding of the welding process and pertained to evaluate residual stress especially bead-on-plate 316L stainless steel welding.

Welding process in FEM is typically modelled as a moving heat source over a solid. The heat source can be modelled as a point heat source (Van Elsen et al., 2007; Dragi and Ivana, 2009; Darmadi et al., 2011). Point heat source is a heat load with value equal to generated heat $\dot{q}$ ($Js^{-1}$) over a nodal at the solid. Heat source may be

modelled as a surface heat source $\dot{q}''$ ($Jm^{-2}s^{-1}$) (Darmadi et al., 2011; Chai et al., 2003; Lu et al., 2004; Dean and Hidekazu, 2006). Surface heat source is a heat flux that is a heat generated over certain area. The heat flux can be uniformly distributed (Darmadi et al., 2011) or distributed according to Gaussian distribution. Heat source can also be represented as a volumetric heat source $\dot{q}'''$ ($Jm^{-3}s^{-1}$) (Lei et al., 2006; Shan et al., 2009; Darmadi, 2011b; Darmadi et al., 2012b). Volumetric heat source is a body heat load applies at a certain volume. As in surface heat source, the volumetric heat source can be uniformly distributed or distributed according to a certain pattern. The most prominent volumetric distributed heat source is Goldak's volumetric heat source model (Goldak et al., 1984). Heat intensity at certain volume for Goldak's model can be expressed as a function of maximum volumetric heat at the heat source centre $\dot{q}_o'''$, heat source parameters ($r_x$, $r_y$, $r_z$) and its relative position to heat source centre ($x$, $y$, $\zeta$) as shown in equation (1).

$$\dot{q}'''_{(x,y,\zeta)} = \frac{6\sqrt{3}\dot{q}_o'''}{\pi\sqrt{\pi}r_x r_y r_z} e^{-\left(\frac{3x^2}{r_x^2}+\frac{3y^2}{r_y^2}+\frac{3\zeta^2}{r_z^2}\right)} \tag{1}$$

In this paper, thermal load was modelled using combination of Goldak's heat source model and uniform temperature load. Goldak's heat source was used to represent heat transferred to base metal by welding torch and uniform temperature load represented melted filler metal.

## 2 Method

The secondary data and welding procedure provided by European Network on Neutron Techniques Standardization for Structural Integrity (NeT) were used. Those data can be accessed freely at https://odin.jrc.ec.europa.eu after simple registration (Truman and Smith, 2009; *Protocol for Phase 2 Finite Element Simulation on the NeT Single-bead-on-plate Test Specimen*). Following welding procedure described by NeT, the APDL program was composed to build a FEM model. First was modelled a thermal model of the welding process followed by sequential mechanical model. The predicted results were validated, again using NeT's data in both thermal and mechanical analysis.

### *2.1 Welding procedure by NeT*

The NeT's experimental work was carried out using bead-on-plate (bop) welding. Nine thermocouples were attached at different measured points. The welding procedures are summarised in Table 1. Four welding specimens (called as A11, A12, A21 and A22) were produced. A sketch diagram for the welding set up and thermocouple positions are presented in Figure 1. It should be noted that the origin of coordinate system is at the weld stop end. The positions of the thermocouples based on the chosen coordinate system are tabulated in Table 2.

**Table 1** Summary of welding procedure

| |
|---|
| Parent material: |
| Size: (120 x 180 x 17) mm |
| AISI Type 316L Austenitic Stainless Steels |
| Residual stress is relieved using heat treatment |
| Filler: |
| ∅0.8 mm |
| Type: 316S96 |
| Spec: A5.9.93 (ASME); ER316H |
| Welding parameters: |
| Welding process: Tungsten inert gas (TIG) |
| Type: Bead-on-plate |
| Weld length: 60 mm |
| Heat input: 633 J $mm^{-1}$ |
| Welding speed: 2.27 mm $s^{-1}$ |

*Source:* *Protocol for Phase 2 Finite Element Simulation on the NeT Single-bead-on-plate Test Specimen*

**Figure 1** Sketch of welding and coordinate system

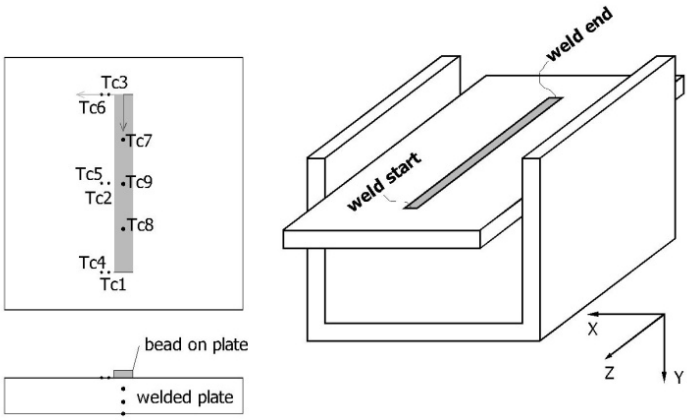


**Table 2** Thermocouple mean-position

| *Thermocouple* | *Mean position (mm)* | | |
|---|---|---|---|
| | *X* | *Y* | *Z* |
| T1 | 8.50 | 1.24 | 60 |
| T2 | 8.00 | 1.20 | 60 |
| T3 | 7.50 | 1.24 | 0 |
| T4 | 11.50 | 1.21 | 60 |

*Source:* *Protocol for Phase 2 Finite Element Simulation on the NeT Single-bead-on-plate Test Specimen*

**Table 2** Thermocouple mean-position

| *Thermocouple* | *Mean position (mm)* | | |
|---|---|---|---|
| | *X* | *Y* | *Z* |
| T5 | 11.50 | 1.23 | 30 |
| T6 | 12.00 | 1.18 | 0 |
| T7 | 0 | 10.50 | 15 |
| T8 | 0 | 4.67 | 46 |
| T9 | 0 | 17.00 | 30 |

*Source: Protocol for Phase 2 Finite Element Simulation on the NeT Single-bead-on-plate Test Specimen*

**Table 3** Base metal properties

| *T(°C)* | *k (W $m^{-1}C^{-1}$)* | *c (J $kg^{-1}C^{-1}$)* | *$\alpha$ (× $10^{-6}C^{-1}$)* | *E (GPa)* |
|---|---|---|---|---|
| 20 | 14.12 | 492 | 14.56 | 195.6 |
| 275 | 17.755 | 523 | 16.7 | 181.125 |
| 550 | 21.67 | 556 | 17.95 | 159.75 |
| 750 | 24.52 | 581 | 18.58 | 137.75 |
| 800 | 25.23 | 587 | 18.72 | 131.4 |
| 900 | 26.66 | 599 | 18.99 | 116.8 |
| 1,100 | 29.5 | 623 | 19.53 | 80 |
| 1,400 | 33.78 | 659 | 20.21 | 2 |

*Source: Protocol for Phase 2 Finite Element Simulation on the NeT Single-bead-on-plate Test Specimen*

**Table 4** Weld metal properties

| *T(°C)* | *k (W $m^{-1}C^{-1}$)* | *c (J $kg^{-1}C^{-1}$)* | *$\alpha$ (× $10^{-6}C^{-1}$)* | *E (GPa)* |
|---|---|---|---|---|
| 20 | 14.12 | 488 | 14.56 | 171 |
| 275 | 17.755 | 532.75 | 16.7 | 151.875 |
| 525 | 21.315 | 576.25 | 17.87 | 133.125 |
| 700 | 23.81 | 589 | 18.43 | 120 |
| 850 | 25.945 | 589 | 18.86 | 102.95 |
| 1,000 | 28.08 | 589 | 19.27 | 83 |
| 1,400 | 33.78 | 589 | 20.21 | 1.7 |

*Source: Protocol for Phase 2 Finite Element Simulation on the NeT Single-bead-on-plate Test Specimen*

Four sets of temperature histories for four specimens were obtained from nine thermocouples. As the thermocouple Tc8 was not pushed far enough into the hole and there was no clear reference to where the data have been recorded, the data from thermocouple Tc8 were not considered. For thermocouple Tc9, the data from specimen A21 were also excluded since they showed a lower temperature and inconsistent with data from other specimens (Smith and Smith, 2009).

The temperature dependent properties of the base metal and welding filler were obtained from the NeT as shown in Tables 3 and 4 respectively. In Figure 2 are shown thermal properties for both metals graphically. The density and Poisson's ratio for both materials are 7,966 kg $m^{-3}$ and 0.294 respectively.

**Figure 2** Materials thermal properties (see online version for colours)

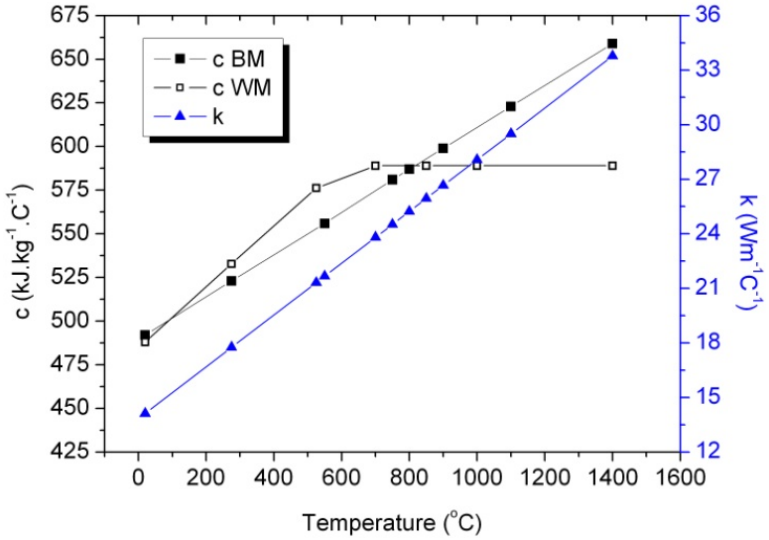


**Figure 3** FEM mesh design (see online version for colours)

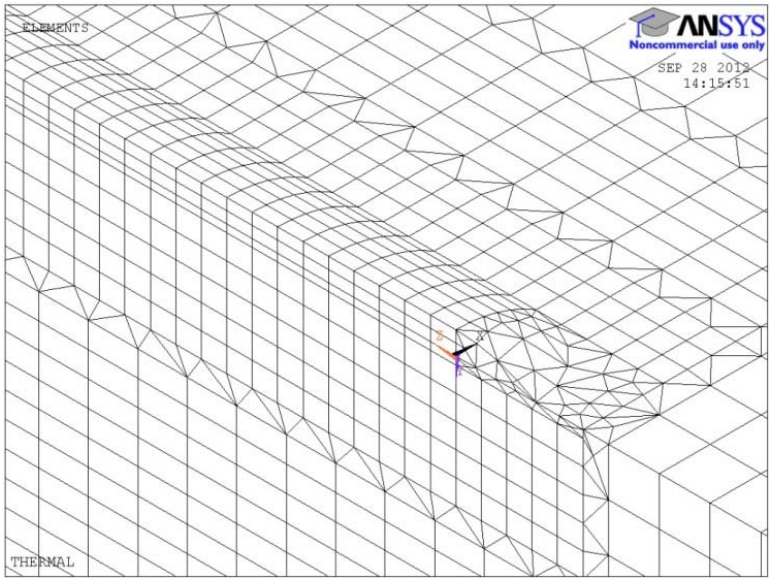

## 2.2 Thermal FEM model

In this paper, finite element model and simulation have been carried out using APDL mode due to its flexibility over the graphics user interface (GUI) mode and it also more suitable to the goal of this research, e.g., improving the knowledge of the welding process. The FEM mesh design is shown in Figure 3 which comprised of 43,639 nodes and 71,128 SOLID70 elements.

**Figure 4** Thermal analysis

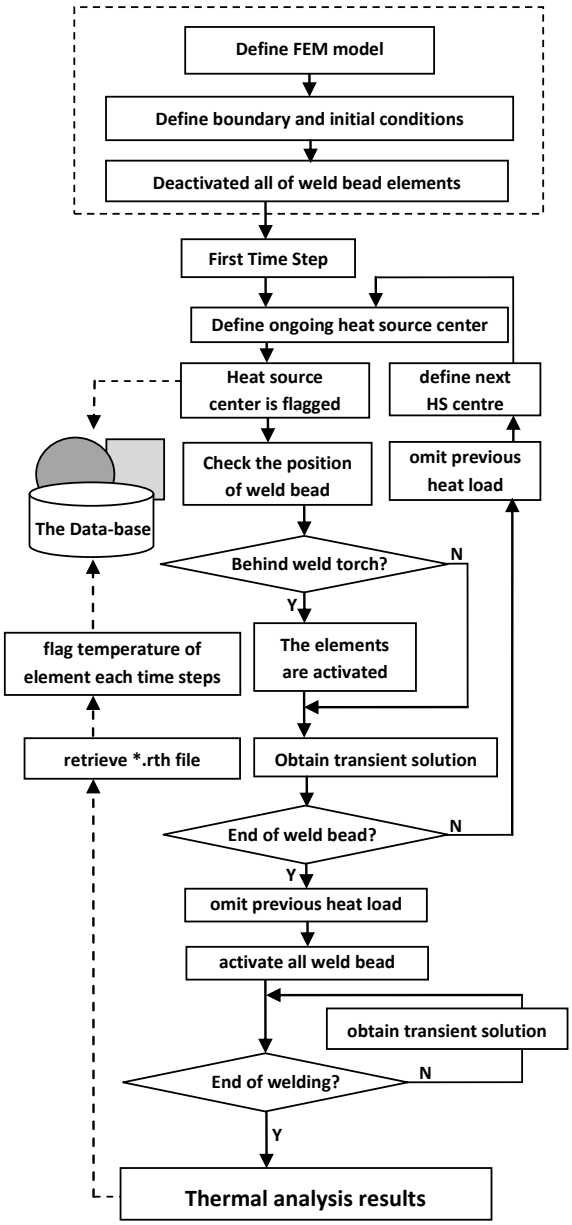

Following a systematic method (Darmadi, 2011b; Darmadi et al., 2012b), heat efficiency was assumed equal to 73%. Heat was divided into two heat sources: semi ellipsoidal Goldak's heat source to model the heat which is transferred to the base metal and uniform temperature load to represent the transferred heat to the melted filler metal. The melted filler metal is superheated and the temperature can reach 2,400°C (Painter and Davies, 1994). The total heat to elevate the temperature of filler metal from the room temperature to 2,400°C is equal to $mc\Delta T$ with m is total mass of weld metal, $c$ is specific heat and $\Delta T$ is temperature elevation. Total heat rate for the weld bead can be obtained using equation (2) with $\rho$, $S$ and $\vec{v}$ represent density, weld length and welding speed respectively. It should be noted that $c$ is temperature dependence and the mean value of each temperature range can be used as a representative.

$$\dot{q}'''_{filler} = \rho c \Delta T \left( \frac{\vec{v}}{S} \right) \tag{2}$$

The total heat rate transferred to the base metal by weld torch should be decreased by the heat rate which is needed to elevate the temperature of filler metal as shown in equation (3) where $E$ is voltage and $I$ is current.

$$\dot{q}''' = 73\% EI - \rho c \Delta T \left( \frac{\vec{v}}{S} \right) \tag{3}$$

Arc dwelling at weld start was considered 3 s and at weld end practically sudden arc extinction was applied (modelled by 0.001 ramped load). Heat lost due to convection and radiation was represented using convection heat transfer coefficient $h_{conv}$ = 5 (watt $m^{-2}K^{-1}$) and surface emissivity $e$ = 0.5. How the thermal analysis was programmed in the ANSYS APDL is shown as a flow chart in Figure 4. To deactivate and activate elements, EKILL and EALIVE commands were used. Heat source centres were defined by nodes which laid on a path where the welding torch moved. Position of weld bead elements were evaluated using *GET command. ANSYS post processor results which were saved in *.rth file were retrieved and saved in a built database using combination of PARRES and PARSAVE commands. This database can be fast and easily retrieved as parameters in the next mechanical analysis.

## *2.3 Sequential mechanical model*

Sequential thermo mechanical analysis was used in this paper since the effect of residual stress to the heat flow is weak, thus it can be neglected (Deaconu, 2007). Temperature histories obtained from thermal analysis were applied as thermal loads in the subsequent mechanical analysis. The mesh in the mechanical analysis should be exactly same as in thermal analysis to facilitate data mapping between thermal and mechanical analysis. Regarding this needs, SOLID45 element model was used in mechanical analysis. SOLID45 has equal geometry with SOLID70 element except for the degree of freedom. Both of them comprise of eight nodes in each cubic elements. Differ elements can be developed by coalescence of nodes. It should be noted that SOLID45 cannot develop pyramid element option, thus in thermal analysis this pyramid element option should be avoided (Darmadi, 2011a). In mechanical analysis, ongoing growing weld bead must match with the growing weld bead in thermal analysis. To fulfil this prerequisite, in thermal analysis the heat source centre for certain time step was flagged and saved in the

database which can be used as a parameter in mechanical analysis. When an element is melted, it will lose its stiffness and current plastic strain. Which elements are melted can be checked in temperature history of each element. Temperature histories of each element in ANSYS is stored in *.rth file. Unfortunately this *.rth is time consumable each time it is retrieved and used as a parameter. To avoid this problem, the temperature history of nodes as a parameter was also obtained from the built database. As it has been mentioned, this data base was created at thermal analysis stage and easily-fast accessed in mechanical analysis. How the sequential thermo-mechanical analysis was performed is shown as a flowchart in Figure 5.

**Figure 5** Sequential mechanical analysis

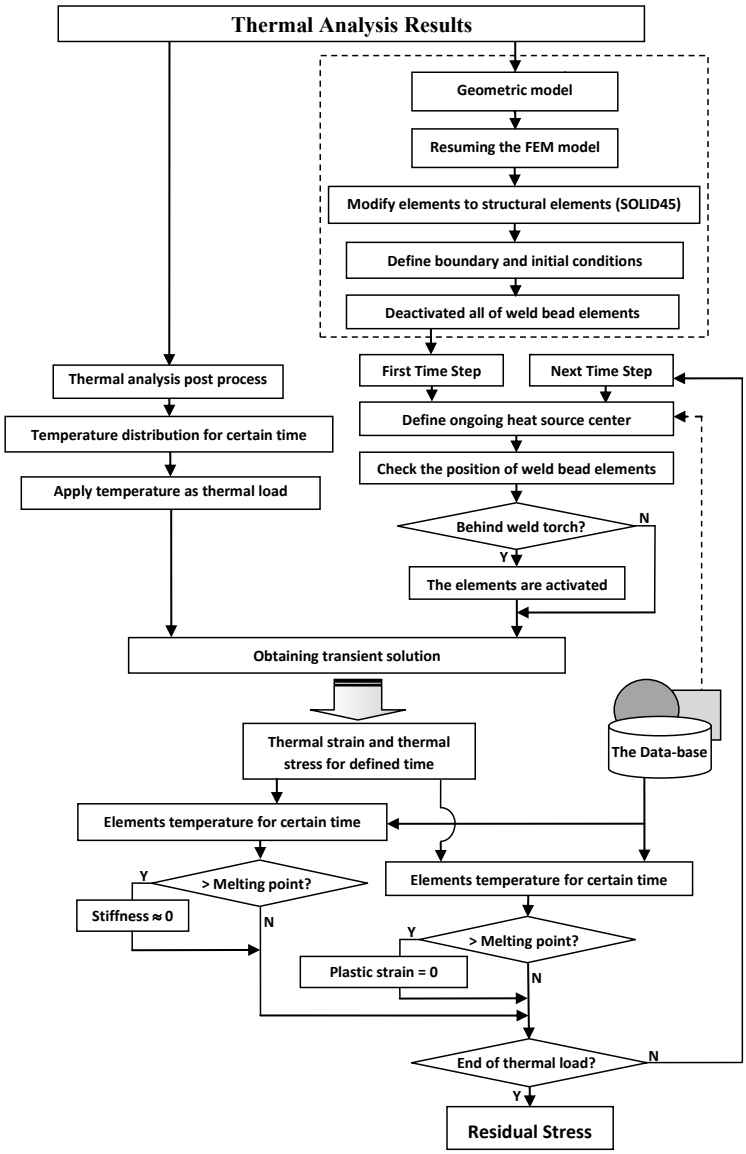

Boundary condition at vice was modelled as constrain at all directions. Symmetry in half area was modelled using constrains $u_x = 0$; $rot_y = rot_z = 0$ means no displacement in $x$ direction and no rotation about axes which are parallel to $y$ axis and $z$ axis. Temperature dependence stress-strain relation for base metal and weld metal are shown in Figures 6 and 7 respectively using data supplied by NeT. In FEM modelling to accommodate those temperature dependence stress-strain relations, a multi-linear kinematic hardening material model was used.

**Figure 6** Temperature dependence stress-strain diagram of base metal (see online version for colours)

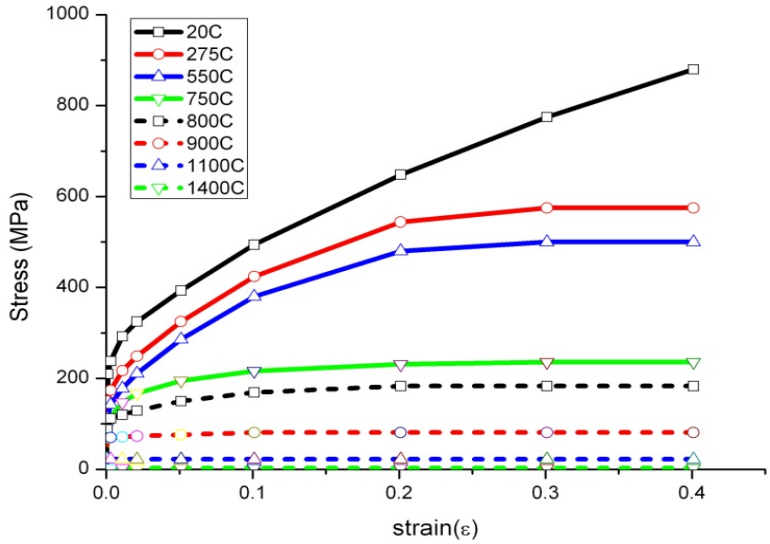


**Figure 7** Temperature dependence stress-strain diagram of weld metal (see online version for colours)

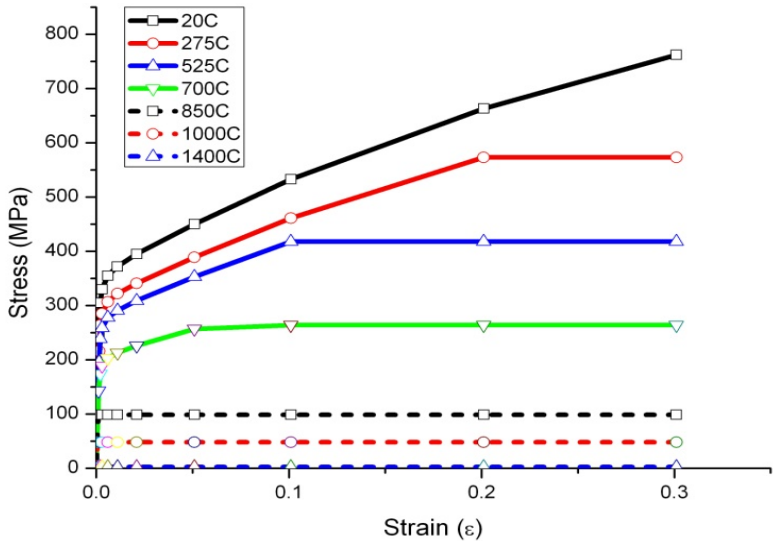

## 4 Results

Results from FEM model which comparable to the experimental result provided by NeT are weld pool shape, temperature histories of selected nodes and residual stresses. Weld pool shape and temperature histories were obtained from thermal analysis while residual stresses were derived from sequential mechanical analysis.

**Figure 8** Weld pool shape, (a) experimental (*Protocol for Phase 2 Finite Element Simulation on the NeT Single-bead-on-plate Test Specimen*) and (b) predicted (see online version for colours)

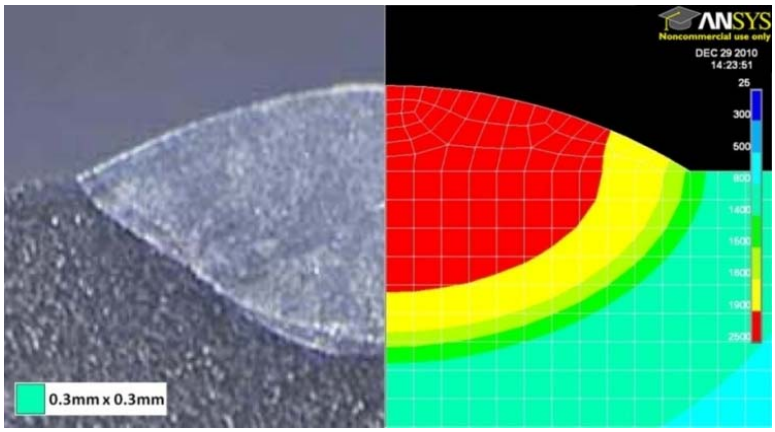


(a) (b)

**Figure 9** Temperature histories for location of thermocouple Tc1 and Tc4 (refer to Figure 1) (see online version for colours)

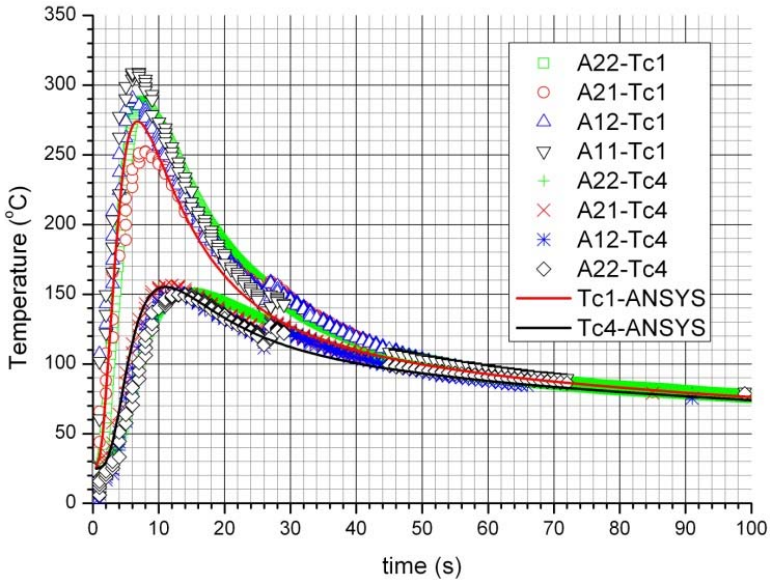

**Figure 10** Temperature histories for location of thermocouple Tc2 and Tc5 (refer to Figure 1) (see online version for colours)

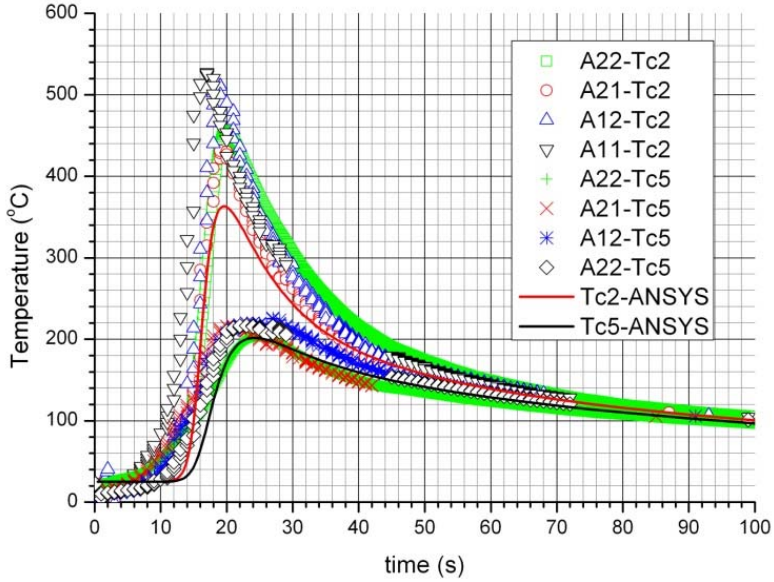


**Figure 11** Temperature histories for location of thermocouple Tc3 and Tc6 (refer to Figure 1) (see online version for colours)

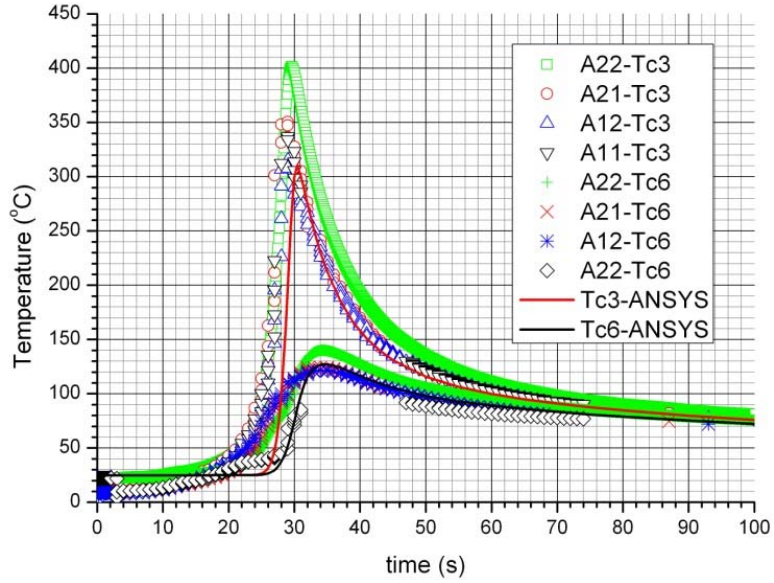

**Figure 12** Temperature histories for location of thermocouple Tc7 (refer to Figure 1) (see online version for colours)

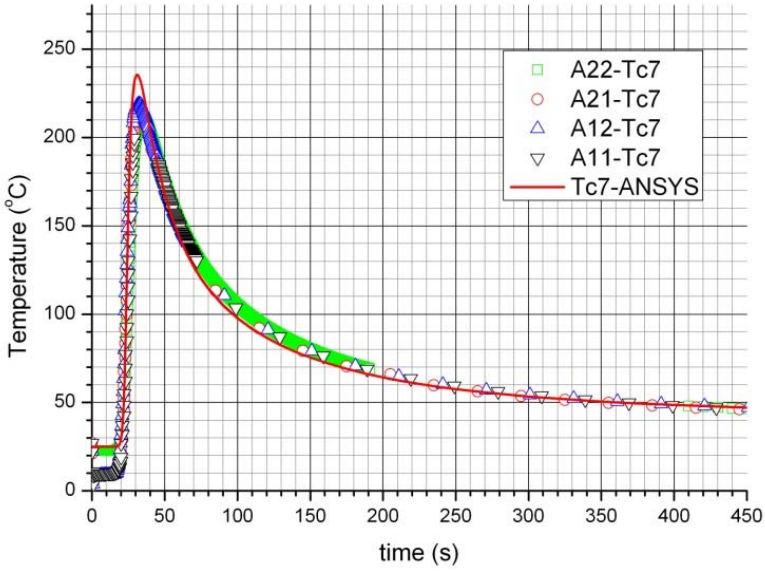


**Figure 13** Temperature histories for location of thermocouple Tc9 (refer to Figure 1) (see online version for colours)

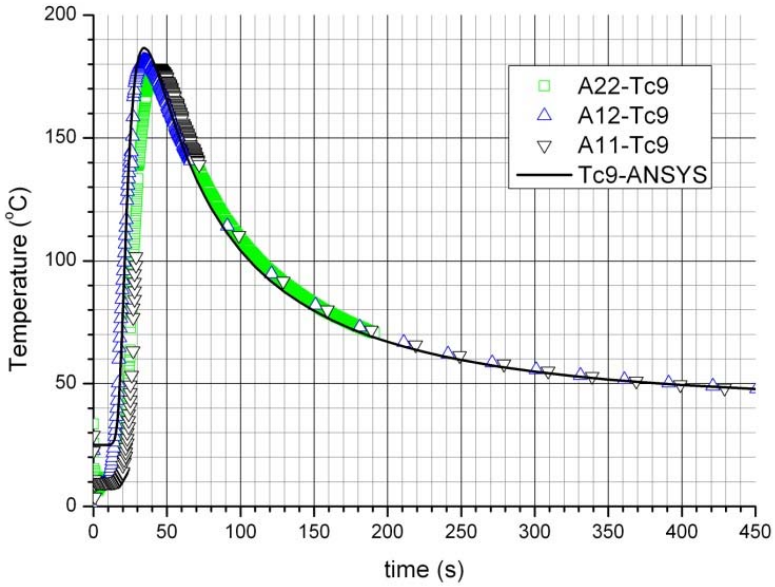

Predicted weld pool shape is represented by isothermal contour of melting temperature which compared to experimental result as shown in Figure 8. Predicted temperature histories of selected nodes which represented thermocouples are shown in Figures 9–13.

**Figure 14** Longitudinal residual stress ($\sigma_z$) distribution (see online version for colours)

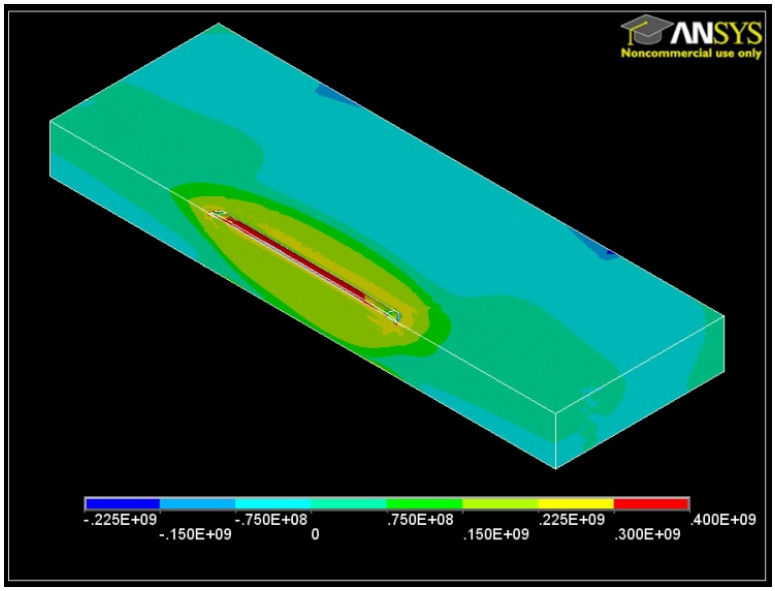


**Figure 15** Transversal residual stress ($\sigma_x$) distribution (see online version for colours)

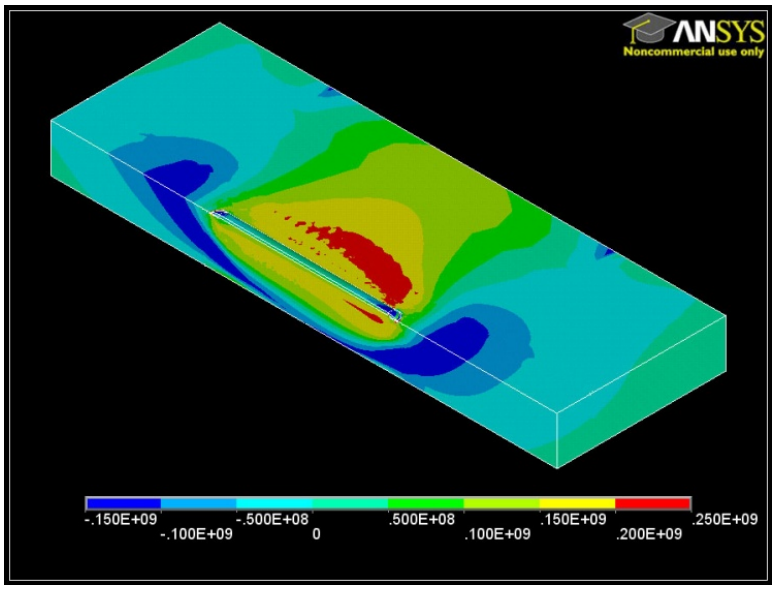

FEM's residual stresses prediction are presented in Figures 14–17. Figure 14 shows distribution of longitudinal residual stress whilst Figure 15 describes transversal residual stress both in isometric view. Longitudinal residual stress distribution in mid cross section is shown in Figure 16 and transversal residual stress distribution in symmetric area is shown in Figure 17. Longitudinal residual stress data from a path 2 mm under top surface as shown in Figure 16 were compared to NeT's experimental results and represented in Figure 18. Figures 19 and 20 show transversal residual stress distribution obtained from FEM prediction and NeT's from 2 mm and 3 mm paths under top surface respectively. Those paths are shown in Figure 17.

## 5 Discussion

FEM thermal analysis followed a logic was discussed in Section 2.2 and used parameters have been described in Section 2.1. Using a model with the above mentioned logic and parameters, quiet good predicted weld-pool and temperature histories at thermocouples can be provided as shown in Figures 8–13. Weld-pool shape was predicted using isothermal temperature field where the temperature is above the melting temperature (1,400°C). The confirmed thermal histories and temperature field clarify the correctness of the thermal model.

It should be noted that there are four different specimens namely A11, A12, A21 and A22 were produced by NeT. It must be some variations from aimed values especially the thermocouple position, and the positions listed in Table 2 are the mean values. Furthermore, the welding itself is a 'noisy' process that although the welding parameters were kept constant small deviation must exist. That is why the measured temperature histories show variations as it can be seen in Figures 9–13. Deviation especially the peak temperature is more significant for closer thermocouple as shown by the measured temperature histories of Tc1, Tc2 and Tc3. The ambient temperature 25°C was considered as the initial temperature of the base metal. It should be noted that the measured Tc7 and Tc9 showed lower base metal initial temperature which in turn caused a bit higher predicted peak temperature. The lower predicted peak temperature of Tc2 is may caused by radiation of welding torch which was not modelled in FEM.

For nearly equal x values (Tc1, Tc2 and Tc3) the peak temperature of mid field thermocouple was higher. The Tc2 was heated by heat source before and after the heat source arrive at Z parallel to Tc2. For Tc1 and Tc3 (weld start and weld end thermocouples) the thermocouple was heated after and before the heat source parallel to these thermocouples respectively. This phenomenon confirmed by FEM prediction and temperature histories measurement.

FEM sequential mechanical analysis followed logic discussed in Section 2.3. It can be seen from Figures 16 and 17 that high tensile longitudinal or transversal stress close to the weld bead was balanced by compressive stress in the area away from the weld bead.

**Figure 16** A selected path for validating longitudinal residual stress ($\sigma_z$) (see online version for colours)

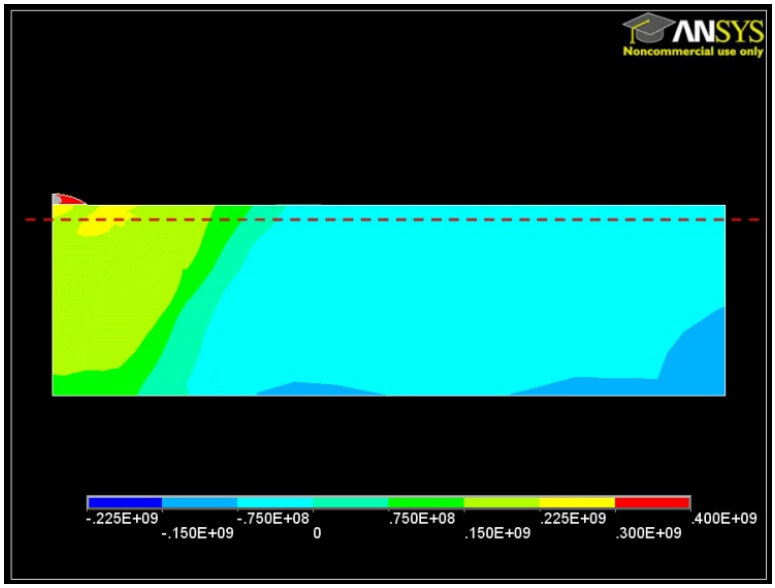


**Figure 17** Selected paths for transversal residual stress ($\sigma_x$) validation (see online version for colours)

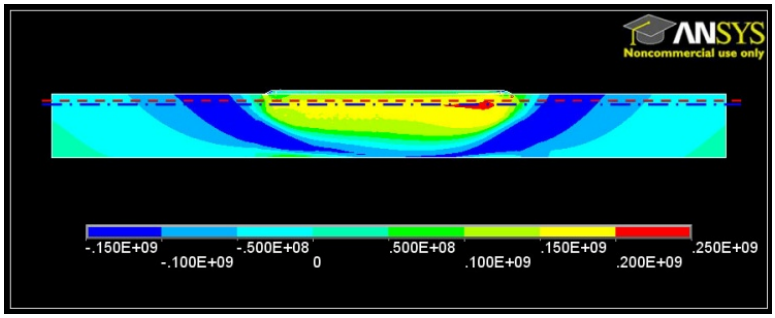


Experiment results for residual stress were provided by some participants in NeT consortium, those are

1 Joint Research Centre, Institute for Energy, The Netherlands – JRC (Ohms et al., 2009)

2 Nuclear Physics Institute, Czech Republic – NPI (Smith and Smith, 2009)

3 Materials Engineering, The Open University, England – OU (Pratihar et al., 2009)

4 Heinz Maier-Leibnitz Institute – HMI (Hofmann and Wimpory, 2009).

All of those participants used neutron diffraction for residual stress measurement and the results were used to validate FEM prediction discussed in this paper.

**Figure 18** Predicted and measured longitudinal residual stress ($\sigma_z$) distribution (see online version for colours)

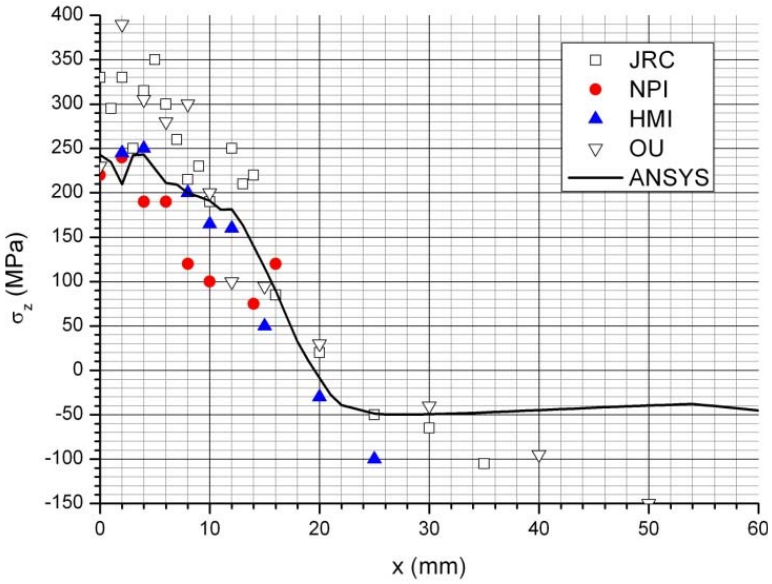


Figure 18 shows longitudinal residual stress of FEM predictions compared to measurements by those four participants. Since the welding was symmetric only half part is shown in the figure.

Considering the experimental results from Figure 18 it can be seen that the data have exhibited a wide degree of scatter. This again demonstrated a fact that the welding is a noisy process. Bouchard (2008) comprehensively discussed this NeT's wide degree of scatter data and introduce what is called as 'innate scatter' that described how differences in residual stress measurements can arise between nominally identical welds. Basically the source of this scatter is the weldment itself and the measurement techniques. For the neutron diffractions, the error is around 10% of material yield stress and for near and within weld metal this error will be higher owing to plastic anisotrophy, texture and compositional effects. Regarding these facts it can be understood why the measurement results were scattered and it can be said that the FEM prediction in Figure 18 agree quiet well with measurement results especially with HMI's.

Figures 19 and 20 show transversal residual stress on 2 mm and 3 mm paths respectively (see Figure 17 for the paths). It should be noted that the weld end was laid on the origin of coordinate system and the weld line spanned to z = 60 mm (Figure 1) where the weld was started. HMI did not report any result for the 2 mm path. The *x* coordinates axis in Figures 19 and 20 are in reverse order to meet the coordinate configuration in Figures 1 and 17. FEM predicted high transversal residual stress at *z* equal to the weld bead on both paths. The predicted transversal stress was around 200 MPa and varied depended on *z* position. This transversal residual stress was little bit lower than longitudinal residual stress close to the weld bead (around 240 MPa). The peak transversal stress at *z* = 60 mm in Figure 19 was caused by 3 s of arc dwelling at weld start. In 3 mm path this peak transversal stress was not exhibited since it far enough from the melted base metal (see Figure 8 for predicted weld pool). Comparing predicted and

measured transversal residual stress in Figure 19, it can be concluded that FEM prediction agree very well with measured results. On the 3 mm path only HMI and JRC reported residual stress distribution (see Figure 20) and again the FEM prediction using the discussed approach can give well-matched result.

**Figure 19** Predicted and measured transversal residual stress ($\sigma_x$) distribution at a path 2 mm under the plate top surface (see online version for colours)

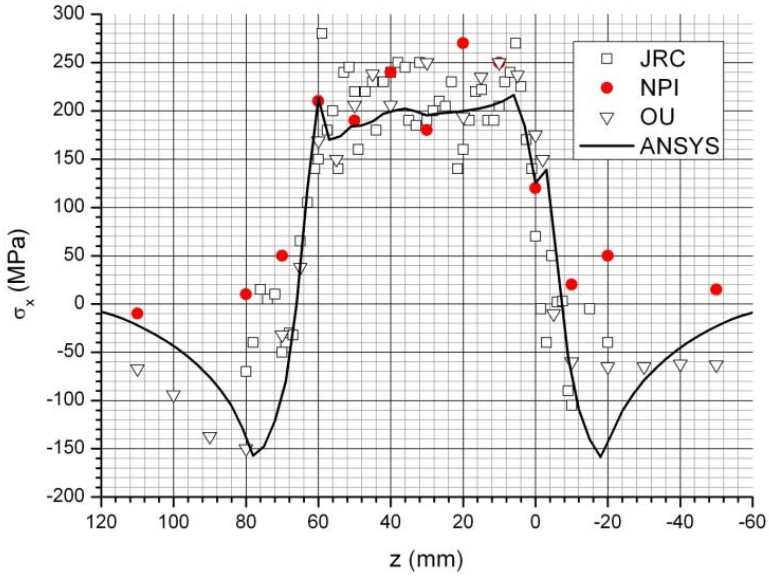


**Figure 20** Predicted and measured transversal residual stress ($\sigma_x$) distribution at a path 3 mm under the plate top surface (see online version for colours)

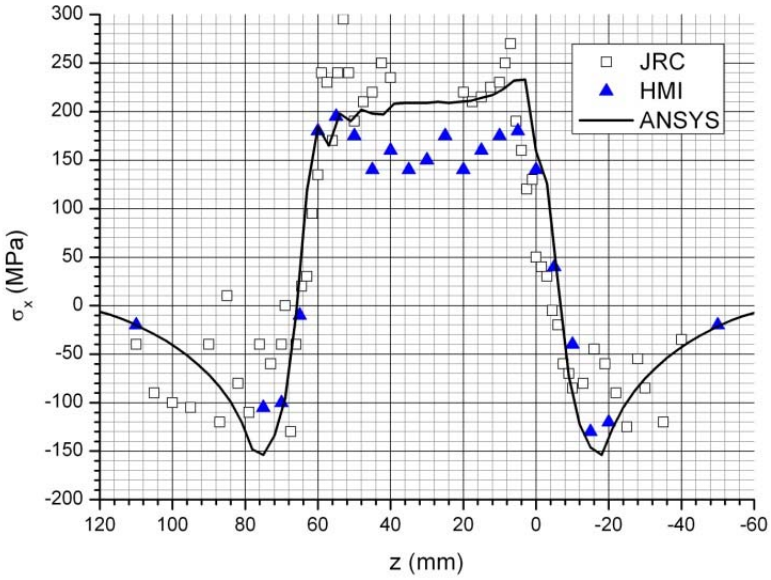

## 6 Conclusions

The moving heat source from welding torch can be well modelled by mixed mode of temperature load which represent melting filler metal and Goldak's volumetric heat load.

Using the mixed mode heat source model, well-matched thermal result can be obtained as shown by temperature histories at thermocouples position and weld-pool shape. Applying the previous well-matched thermal results as a temperature load in the consecutive mechanical FEM model, accurate residual stress prediction can be provided. When melting takes places, the materials lose it stiffness and previous plastic strain that should be accommodated in the FEM model. This idea can be applied in the APDL mode using a built database which contains needed parameters. This validated result has also confirmed the minor effect of mechanical on thermal results, thus uncoupled thermo-mechanical analysis can provide close enough prediction of residual stress.

Overall, it can be said that the FEM modelling approach used in this paper could well perform thermo-mechanical welding of the bead on plate welding.

## References

Akbari, D. and Sattari-Far, I. (2009) 'Effect of the welding heat input on residual stresses in butt-welds of dissimilar pipe joints', *International Journal of Pressure Vessels and Piping*, Vol. 86, No. 11, pp.769–776.

Anawa, E.M. and Olabi, A.G. (2008) 'Control of welding residual stress for dissimilar laser welded materials', *Journal of Materials Processing Technology*, Vol. 204, No. 1, pp.22–33.

Bouchard, P.J. (2008) 'Code characterisation of weld residual stress levels and the problem of innate scatter', *International Journal of Pressure Vessels and Piping*, Vol. 85, No. 3, pp.152–165.

Chai, Z., Zhao, H. and Lu, A. (2003) 'Efficient finite element approach for modeling of actual welded structures', *Science and Technology of Welding and Joining*, Vol. 8, No. 3, pp.195–204.

Darmadi, D.B. (2011a) 'Study of residual stress mechanism using three elasto-plastic bars model', *Asian Transaction*, Vol. 1, No. 5, pp.76–80.

Darmadi, D.B. (2011b) 'Validating the accuracy of heat source model via temperature histories and temperature field in bead-on-plate welding', *International Journal of Engineering and Technology*, Vol. 11, No. 5, pp.12–20.

Darmadi, D.B., Norrish, J. and Tieu, A.K. (2011) 'Analytic and finite element solutions for temperature profiles in welding using varied heat source models', *World Academy of Science, Engineering and Technology*, Vol. 81, No. 57, pp.154–162.

Darmadi, D.B., Marimuthu, M., Tieu, K. and Norrish, J. (2012a) 'Numerical prediction of residual stresses in 316L bead on plate welds', *15th International Conferences on Advanced in Materials & Processing Technology (AMPT)*, Australia, Paper Id: 11355.

Darmadi, D.B., Tieu, A.K. and Norrish, J. (2012b) 'A validated thermal model of bead-on-plate welding', *Journal of Heat and Mass Transfer*, Vol. 48, No. 7, pp.1219–1230.

Deaconu, V. (2007) 'Finite element modelling of residual stress – a powerful tool in the aid of structural integrity assessment of welding structure', *5th Int. Conference Structural Integrity of Welded Structures*.

Dean, D. and Hidekazu, M. (2006) 'Prediction of welding residual stress in multi-pass butt-welded modified 9Cr-1Mo steel pipe considering phase transformation effects', *Computational Materials Science*, Vol. 37, No. 3, pp.209–219.

Dragi, S. and Ivana, V. (2009) 'Finite element analysis of residual stress in butt welding two similar plates', *Scientific Technical Review*, Vol. 59, No. 1, pp.57–60.

Gannon, L., Liu, Y., Pegg, N. and Smith, M. (2010) 'Effect of welding sequence on residual stress and distortion in flat-bar stiffened plates', *Marine Structures*, Vol. 23, No. 3, pp.385–404.

Gannon, L., Liu, Y., Pegg, N. and Smith, M.J. (2012) 'Effect of welding-induced residual stress and distortion on ship hull girder ultimate strength', *Marine Structures*, Vol. 28, No. 1, pp.25–49.

Goldak, J. and Asadi, M. (2011) 'Computational weld mechanics and optimization of welding procedures, welds, and welded structures', *Transaction of JWRI*, Special Issue on WSE2011, No. 1, pp.55–60.

Goldak, J., Chakravarti, A. and Bibby, M. (1984) 'A new finite element model for heat sources', *Metallurgical Transactions B*, Vol. 15B, No. 2, pp.299–305.

Hofmann, M. and Wimpory, R.C. (2009) 'NeT TG1: residual stress analysis on a single bead weld on a steel plate using neutron diffraction at the new engineering instrument 'STRESS-SPEC'', *International Journal of Pressure Vessels and Piping*, Vol. 86, No. 1, pp.122–125.

Lei, Y-c., Yu, W-x., Li, C-h. and Cheng, X-n. (2006) 'Simulation on temperature field of TIG welding of cooper without preheating', *Transaction of Nonferrous Metals Society of China*, Vol. 16, No. 2, pp.838–843.

Lu, F., You, S. and Li, Y. (2004) 'Modeling and finite element analysis on GTAW arc and weld pool', *Computational Materials Science*, Vol. 29, No. 3, pp.371–378.

Moraitis, G.A. and Labeas, G.N. (2008) 'Residual stress and distortion calculation of laser beam welding for aluminum lap joints', *Journal of Materials Processing Technology*, Vol. 198, Nos. 1–3, pp.260–269.

Murakawa, H., Beres, M., Davies, C.M., Rashed, S., Vega, A., Tsunori, M., Nikbin, K.M. and Dye, D. (2010) 'Effect of low trans-formation temperature weld filler metal on welding residual stress', *Science and Technology of Welding and Joining*, Vol. 15, No. 5, pp.393–399.

Norrish, J. (2006) 'Advance welding processes – technology and process control', *Woodhead Publishing in Materials*.

Ohms, C., Wimpory, R.C., Katsareas, D.E. and Youtsos, A.G. (2009) 'NeT TG1: residual stress assessment by neutron diffraction and finite element modeling on a single bead weld on a steel plate', *International Journal of Pressure Vessels and Piping*, Vol. 86, No. 1, pp.63–72.

Painter, M.J. and Davies, M.H. (1994) *Numerical Modeling of the Gas Metal Arc Welding Process*, Annual Report – CRC Project: 93.04.

Pratihar, S., Turski, M., Edwards, L. and Bouchard, P.J. (2009) 'Neutron diffraction residual stress measurements in a 316L stainless steel bead-on-plate weld specimen', *International Journal of Pressure Vessels and Piping*, Vol. 86, No. 1, pp.13–19.

*Protocol for Phase 2 Finite Element Simulation on the NeT Single-bead-on-plate Test Specimen* [online] https://odin.jrc.ec.europa.eu (accessed 17 August 2012).

Shan, X., Davies, C.M., Wangsdan, T., O'Dowd, N.P. and Nikbin, K.M. (2009) 'Thermo-mechanical modeling of a single-bead-on-plate weld using the finite element method', *International Journal of Pressure Vessels and Piping*, Vol. 86, No. 1, pp.110–121.

Smith, D.G. (2009) *Laser Welding of Casting to Minimize Distortion*, No. EP 2 065 118 A1, European Patent Application.

Smith, M.C. and Smith, A.C. (2009) 'NeT bead-on-plate round robin: comparison of residual stress predictions and measurements', *International Journal of Pressure Vessels and Piping*, Vol. 86, No. 1, pp.79–95.

Sudhakaran, R., Vel Murugan, V. and Siva Sakthivel, P.S. (2010) 'Optimization of process parameters to minimize angular distortion in gas tungsten arc welded stainless steel 202 grade plates using genetic algorithms', *International Journal of Engineering Science and Technology*, Vol. 2, No. 5, pp.731–748.

Sudheesh, R.S. and Siva Prasad, N. (2011) 'Finite element study of residual stresses and distortion in arc welding with a trailing liquid nitrogen heat sink', *International Journal of Numerical Methods for Heat & Fluid Flow*, Vol. 21, No. 8, pp.1050–1065.

Truman, C.E. and Smith, M.C. (2009) 'The NeT residual stress measurement and modeling round robin on a single weld bead-on-plate specimen', *International Journal of Pressure Vessels and Piping*, Vol. 84, No. 1, pp.1–2.

Van Elsen, M., Baelmans, M., Mercelis, P. and Kurth, J.P. (2007) 'Solution for modeling moving heat source in a semi-infinite medium and application to laser material processing', *International Journal of Heat and Mass Transfer*, Vol. 50, No. 24, pp.4872–4882.

Xu, D., Liu, X.S., Wang, P., Yang, J.G. and Fang, H.Y. (2009) 'New technique to control welding buckling distortion and residual stress with non-contact electromagnetic impact', *Science and Technology of Welding and Joining*, Vol. 14, No. 8, pp.753–759.

Xu, J., Chen, L. and Ni, C. (2007) 'Effect of vibratory weld conditioning on the residual stresses and distortion in multi-pass girth-butt welded pipes', *Pressure Vessels and Piping*, Vol. 84, No. 5, pp.298–303.